

## Constant-potential amperometric detector for carbohydrates at a nickel(III) oxide electrode for micro-scale flow-injection analysis and high-performance liquid chromatography

MASASHI GOTO\*

Department of Pharmaceutical Analytical Chemistry, Gifu Pharmaceutical University, 5–6–1 Mitahora-Higashi, Gifu 502 (Japan)

and

HIROYOSHI MIYAHARA and DAIDO ISHII

Department of Applied Chemistry, Faculty of Engineering, Nagoya University, Chikusa-ku, Nagoya 464 (Japan)

---

### ABSTRACT

A constant-potential amperometric detector for carbohydrates based on oxidation at an active nickel(III) oxide electrode for micro flow-injection analysis (micro-FIA) and micro high-performance liquid chromatography (micro-HPLC) was developed. The active nickel(III) oxide is formed *in situ* on the electrode surface at potentials near *ca.* 0.5 V vs. Ag/AgCl. The nickel(III) surface acts as a strong oxidant and reacts with the carbohydrate by hydrogen atom abstraction to yield a radical. A tubular-type electrolytic cell was constructed by inserting nickel wire of diameter 25 or 50  $\mu\text{m}$  and length *ca.* 5 mm into the fused-silica tube (50 or 100  $\mu\text{m}$  I.D.). The effective cell volume was less than *ca.* 30 nL. The cell was successfully applied to the detection of various sugars such as aldopentoses, aldohexoses, ketohexoses, sugar alcohols, disaccharides and trisaccharides. The detection limit of micro-FIA was 0.1 ng (signal-to-noise ratio = 3) for glucose.

---

### INTRODUCTION

Liquid chromatography has become a well established technique for the separation of carbohydrates. Unfortunately, the absence of a strongly absorbing chromophore in carbohydrates restricts the use of direct UV-visible detection. Refractive index detection, the most generally used mode, often lacks sensitivity. Recently, improvements in sensitivity have been attempted by the development of electrochemical detectors based on the direct or catalytic electrooxidation of carbohydrates in highly basic solution<sup>1–13</sup>. In order to reduce the large overpotential for carbohydrate oxidation, various working electrode materials have been used. Electrochemical detectors for carbohydrates can be divided into two groups. The first

group employs platinum<sup>1-3</sup> or gold<sup>4-7</sup> electrodes on which the carbohydrates adsorb and subsequently undergo relatively facile dehydrogenation/oxidation. However, because of the surface cleaning and regeneration steps necessary to obtain a stable response, simple constant-potential operation is not possible, and double- or triple-pulse potential waveforms are required. The detection limits for carbohydrates with platinum and gold electrodes are about 100 and 10 ng, respectively. The second group employs catalytic electrodes using an oxidizable metal such as nickel<sup>8-10</sup>, copper<sup>11</sup> and silver<sup>11</sup>, or containing a surface-attached electron-transfer mediator such as cobalt phthalocyanine<sup>12,13</sup>. For these, the lowest detection limits (1 ng for monosaccharides and 5 ng for oligosaccharides) have been found with nickel electrodes. More recently, a copper-based chemically modified electrode has been developed for a constant-potential amperometric detector<sup>14</sup>. Such an electrode was prepared by coating a glassy carbon electrode with a copper(II) layer that catalyses the oxidation of carbohydrates when a potential sufficiently positive to generate copper(III) is applied. Detection limits at the subnanogram level (0.22 ng for glucose) have been reported with this type of detector. However, none of the electrochemical detectors reported are suitable for micro-scale flow-injection analysis (micro-FIA) or high-performance liquid chromatography (micro-HPLC) because of the relatively large cell volume.

In this work, an electrolytic cell with an extremely small volume for a constant-potential amperometric detector based on oxidation at an active nickel(III) oxide electrode was constructed by using a nickel wire of diameter 25 or 50  $\mu\text{m}$  and applied in micro-FIA and micro-HPLC.

## EXPERIMENTAL

### *Reagents*

Stock solutions of 21 kinds of carbohydrates, purchased from Wako or Aldrich, were prepared fresh daily in deionized water and, just prior to use, were adjusted to the desired concentration. Supporting electrolyte solution was prepared from carbonate-free sodium hydroxide and deionized water.

### *Apparatus*

Cyclic voltammetry (CV) was performed with a new cyclic voltammetric analyser (Yanagimoto, VMA-010) and an *X-Y* recorder (Yokogawa, 3086). A schematic diagram of the micro-HPLC apparatus is shown in Fig. 1. A micro-feeder (Azuma Denki, FM-2) and two micro-syringes (Ito, GAN-050) were used for feeding the mobile phase (carrier) and the electrolyte solution to reduce pulsations in the flow. A micro-valve injector (Nihon Bunko, ML-422; 20 nl) was used for sample injection. The fundamental construction of the tubular-type electrolytic cell, which is similar to that of a carbon fibre working electrode<sup>15</sup>, is shown in Fig. 2. A nickel wire of diameter 25 or 50  $\mu\text{m}$  and length 5mm was inserted into the fused-silica tube (50 or 100  $\mu\text{m}$  I.D., respectively) to serve as the working electrode. A silver/silver chloride and a platinum counter electrode were placed outside the tube near the outlet of the solution. The effective cell volume was less than *ca.* 30 nl.

A voltammetric detector (Yanagimoto, VMD-101) and a recorder (Yokogawa, 3056) were used for constant-potential amperometry. The electrolytic cell was

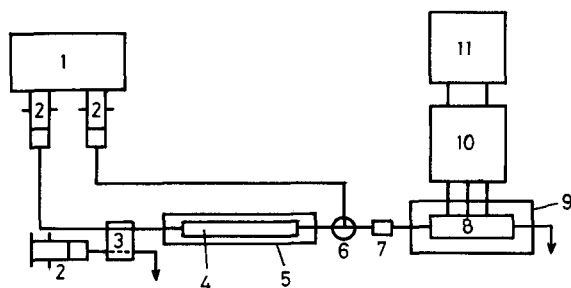


Fig. 1. Schematic diagram of apparatus for micro-HPLC. 1 = Micro-feeder; 2 = micro-syringe; 3 = valve injector (0.02  $\mu$ l); 4 = micro-separation column; 5 = water-bath; 6 = mixing joint; 7 = mixing column; 8 = electrolytic flow cell; 9 = heater; 10 = potentiostat; 11 = recorder.

thermostated by using a column heater (Sugai Kagaku, U-620). Laboratory-made micro-separation columns packed with Shodex Ionpak KS-801 (247 mm  $\times$  0.35 mm I.D. + 217 mm  $\times$  0.35 mm I.D.) and SAX (100 mm  $\times$  0.25 mm I.D. + 100 mm  $\times$  0.25 mm I.D.) were used for size-exclusion and ion-exchange chromatography of carbohydrates, respectively. For ion-exchange chromatography, the electrolyte solution was mixed before the column instead of after the column. Micro-FIA experiments were carried out by removing the micro-separation columns.

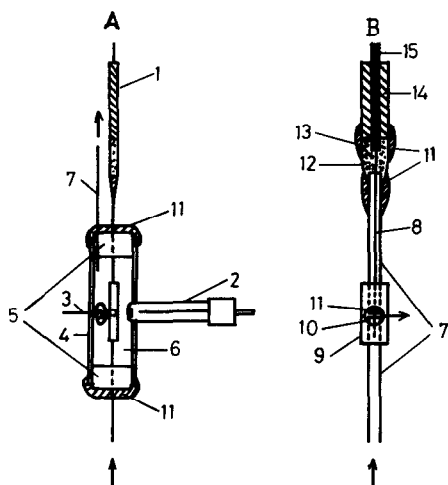


Fig. 2. Structure of electrolytic flow cell of tubular type. (A) Whole cell; (B) detail of working micro-electrode. 1 = Working electrode; 2 = reference electrode (Ag/AgCl); 3 = counter electrode (Pt wire); 4 = acrylic tube; 5 = rubber cup; 6 = electrolyte solution (mobile phase); 7 = fused-silica tube (50 or 100  $\mu$ m I.D.); 8 = Ni wire (diameter 25 or 50  $\mu$ m, length 5 mm); 9 = PTFE tube (0.1 mm I.D., 2 mm O.D.); 10 = hole; 11 = adhesive resin; 12 = glass pipette; 13 = silver paste; 14 = insulator; 15 = electric wire.

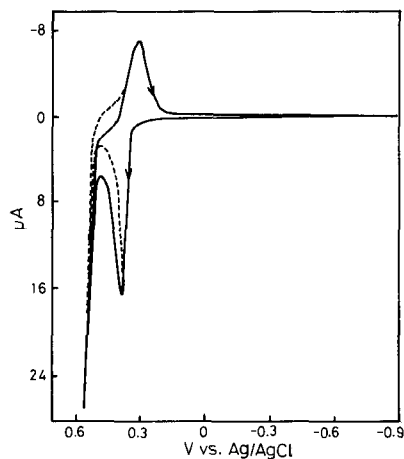
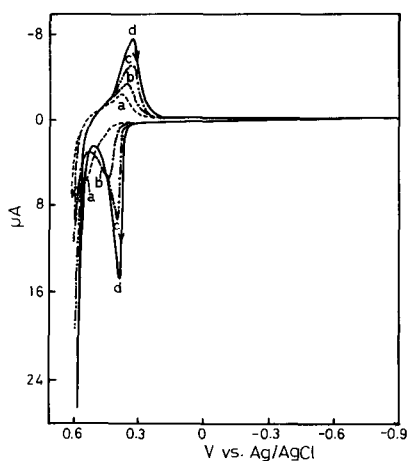


Fig. 3. Consecutive cyclic voltammograms of nickel micro-electrode itself in 0.5 M NaOH. Order of potential scans: (a) 1st; (b) 2nd; (c) 5th; (d) multiple scans. Working electrode, Ni wire (diameter 50  $\mu\text{m}$ , length 5 mm); potential scan rate, 100 mV/s.

Fig. 4. Cyclic voltammogram of glucose in 0.5 M NaOH using a nickel working micro-electrode. Solid line, 1.0 mM glucose; dashed line, 0 mM glucose. Potential scan rate, 100 mV/s.

## RESULTS AND DISCUSSION

### *Electrochemistry*

Cyclic voltammograms obtained for the nickel micro-electrode immersed in oxygen-free 0.5 M NaOH are shown in Fig. 3. During the first scan in the anodic direction, a single, broad oxidation wave with a peak potential of 0.55 V (vs. Ag/AgCl) was observed. This may be due to the oxidation of metallic nickel to a nickel(II) compound. On subsequent scans, this wave gradually increased and shifted to the negative potential side. After more than ten scans, a steady-state cyclic voltammogram, which shows an oxidation wave with a peak potential of 0.38 V and a re-reduction wave with a peak potential of 0.32 V, was observed. The peak height of the oxidation wave at the steady state was proportional to the potential scan rate. This indicates that the wave is due not to the soluble species but to the absorbed species on the electrode. The peak potential of the oxidation wave at the steady state was changed to the negative side at the rate of 60 mV/pH with increasing NaOH concentration in the medium, indicating that  $\text{OH}^-$  is involved in the electrode reaction. In conclusion, the peaks in the steady-state voltammogram correspond to the nearly reversible oneelectron reaction between  $\text{Ni}(\text{OH})_2$  and  $\text{NiO}(\text{OH})$ . Addition of glucose to the above NaOH solution produced a clear increase in the oxidation current, whereas the re-reduction current was almost the same as that obtained without glucose (see Fig. 4). This suggests that nickel in contact with NaOH solution becomes covered with a layer of nickel(II) hydroxide mainly by electrooxidation, from which, at a high enough applied potential,  $\text{NiO}(\text{OH})$  is formed. Acting as a catalyst, this nickel(III) compound may oxidize carbohydrates such as glucose and  $\text{NiO}(\text{OH})$  itself is reduced to  $\text{Ni}(\text{OH})_2$ , which again will be oxidized by the applied potential to give an increased oxidation current, as pointed out by Fleischmann *et al.*<sup>16</sup>

*Micro-FIA*

On the basis of the above CV results, it seemed likely that the amperometric detection of carbohydrates in flow analysis might be able to be carried out at relatively low potentials on the nickel(III) oxide electrode. The hydrodynamic voltammograms for glucose and lactose obtained on the nickel(III) oxide micro-electrode (diameter 25  $\mu\text{m}$ , length 5 mm) are shown in Fig. 5. In this instance, pure water and 0.25  $M$  sodium hydroxide solution were used as the carrier and the electrolyte solution, respectively, each at a flow-rate of 1.1  $\mu\text{l}/\text{min}$  and 0.02  $\mu\text{l}$  of each sample being injected. The maximum electrode responses were observed at a working electrode potential of 0.63  $V$  (vs.  $\text{Ag}/\text{AgCl}$ ), independent of species, and oxygen generation began to occur at about 0.60  $V$  as shown in the dashed line. In order to obtain high sensitivity, a potential of 0.57  $V$ , at which the ratio of peak current to background current was maximum, was chosen as a suitable applied potential for amperometry in this work.

The effect of the flow-rates of the carrier and electrolyte solutions on the electrode response is shown in Fig. 6. In this instance, the ratio of the flow-rate of the carrier (pure water) to that of the electrolyte solution was kept at 1:1 and 1.0  $M$  sodium hydroxide solution was used as the electrolyte solution. The electrode response tended to increase with decreasing flow-rate and to become nearly constant at flow-rates higher than about 2.8  $\mu\text{l}/\text{min}$ . This indicates that a longer contact time of the sample with the electrode is preferable. With respect to the time of analysis, a flow-rate of 1.1  $\mu\text{l}/\text{min}$  was chosen as the most suitable for both the carrier and electrolyte solution in further work.

The effect of alkali concentration in the electrolyte solution on the electrode response was investigated. It was found that the electrode response was a maximum at a sodium hydroxide concentration of about 0.25  $M$ , and the background current

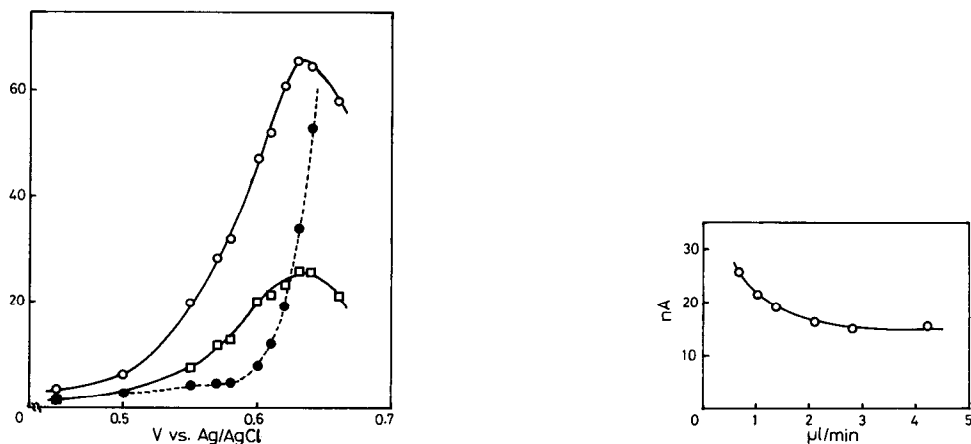


Fig. 5. Relationship between applied potential and peak height in micro-FIA. ( $\circ$ ) 10  $mM$  Glucose sample; ( $\square$ ) 10  $mM$  lactose sample; ( $\bullet$ ) background current. Injection volume, 0.02  $\mu\text{l}$ ; flow-rates of water and 0.25  $M$   $\text{NaOH}$ , both 1.1  $\mu\text{l}/\text{min}$ ; working electrode, Ni wire (diameter 25  $\mu\text{m}$ , length 5 mm).

Fig. 6. Effect of flow-rates of carrier (pure water) and electrolyte solution on peak height. Sample, 10  $mM$  glucose; injection volume, 0.02  $\mu\text{l}$ ; applied potential, 0.57  $V$  vs.  $\text{Ag}/\text{AgCl}$ ;  $\text{NaOH}$  concentration in electrolyte solution, 1.0  $M$ .

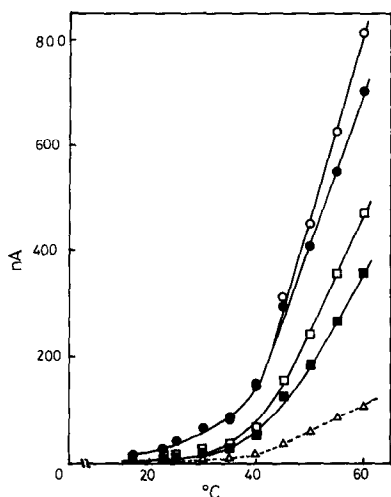


Fig. 7. Effect of detection temperature on peak height. (○) Glucose; (●) arabinose; (□) lactose; (■) raffinose; (△) background current. Concentration of sample, 10 mM each; injection volume, 0.02  $\mu$ l; applied potential, 0.57 V vs. Ag/AgCl; flow-rates of water and 0.25 M NaOH, both 1.1  $\mu$ l/min.

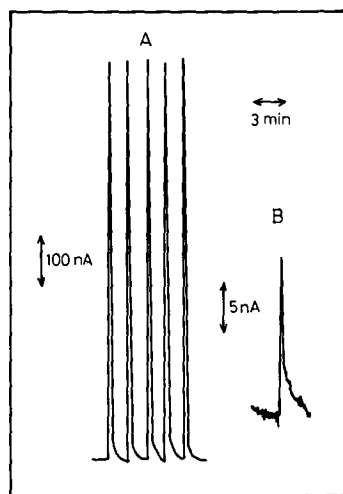


Fig. 8. Typical responses of glucose in micro-FIA. (A) 10 mM; (B) 0.1 mM. Injection volume, 0.02  $\mu$ l; applied potential, 0.57 V vs. Ag/AgCl; flow-rates of water and 0.25 M NaOH, both 1.1  $\mu$ l/min; detection temperature, 60°C.

increased linearly with increasing sodium hydroxide concentration. A sodium hydroxide concentration in the electrolyte solution of 0.25 M was therefore used in further work.

When the temperature of the detector was increased from 17 to 60°C, the electrode response increased dramatically, as shown in Fig. 7. This indicates that the chemical oxidation of carbohydrates by nickel(III) oxide is the rate-limiting step in the proposed detection mode and the temperature increase accelerates the reaction rate. Operation at higher temperatures required a back-pressure to prevent gas production in solution. In the cell construction shown in Fig. 2, gas production did not occur at temperatures up to 60°C. Typical responses of glucose at different concentrations in micro-FIA at a detection temperature of 60°C are shown in Fig. 8. The detection limits of glucose at 30 and 60°C were 0.35 and 0.10 ng (signal-to-noise ratio = 3), respectively, and the peak currents at 30 and 60°C were proportional to the amount of glucose up to 90 ng (25 mM for a sample size of 0.02  $\mu$ l) and 18 ng (5 mM for a sample size of 0.02  $\mu$ l), respectively. A glucose detection limit of 0.1 ng with the proposed micro-detector compares favourably with those for conventional detectors with platinum<sup>2</sup>, gold<sup>7</sup>, nickel<sup>10</sup>, cobalt phthalocyanine<sup>13</sup> and copper-based chemically modified<sup>14</sup> electrodes. For example, Neuburger and Johnson<sup>17</sup> described a coulometric variation of the commercially available pulsed amperometric detector with a gold electrode which improved the glucose detection capability from 315 to 9 ng. This corresponds to a figure of merit 90 times poorer than that obtained here.

The relative standard deviations for the determination of carbohydrates at the 10 mM level with the proposed detector were about 1.5%. The relative intensities with

TABLE I

## RELATIVE INTENSITIES OF RESPONSES FOR VARIOUS CARBOHYDRATES IN MICRO-FIA

Applied potential, 0.57 V vs. Ag/AgCl; flow-rates of water and 0.25 M NaOH, both 1.1  $\mu$ l/min; detection temperature, 30°C.

<i>Species</i>	<i>Compound</i>	<i>Relative intensity</i>
Aldopentoses	Xylose	0.89
	Ribose	0.92
	Arabinose	0.92
Aldohexoses	Glucose	1.00
	Mannose	0.70
	Allose	0.99
	Galactose	1.01
Ketohexoses	Fructose	0.64
	Sorbose	0.60
Deoxysugars	2-Deoxyribose	0.11
	2-Deoxyglucose	0.12
	Fucose (6-deoxygalactose)	0.56
	Rhamnose (6-deoxymannose)	0.30
Sugar alcohols	Ribitol	0.98
	Sorbitol	1.17
	Mannitol	0.96
Glycoside	Methyl-D-glucoside	0.28
Disaccharides	Lactose	0.43
	Sucrose	0.35
	Trehalose	0.23
Trisaccharide	Raffinose	0.33

respect to glucose in equal molar concentrations of the responses for various carbohydrates at a detection temperature of 30°C are summarized in Table I. The relative intensity tended to decrease in the order mono-, di- and trisaccharides. It is clear that the proposed detector can detect not only reducible sugars, but also non-reducible sugars containing sugar alcohols.

### Micro-HPLC

The proposed detector was applied to the detection of carbohydrates separated by micro-HPLC with the micro-separation columns described under Experimental with different separation modes. The results are shown in Fig. 9. In both instances the nickel wire of diameter 25  $\mu$ m and length 5 mm was used as the working electrode, and the detection temperature, the total flow-rate and the sodium hydroxide concentration of the solution in the detector were kept at 60°C, 2.1  $\mu$ l/min and 0.13 M, respectively. Pure water and 0.13 M sodium hydroxide solution were used as the mobile phases for the size-exclusion and ion-exchange modes, respectively. The separation columns for the size-exclusion and ion-exchange modes were kept at 80 and 30°C, respectively, by using a water-bath. It should be noted that the elution orders of the samples investigated were the opposite in the two separation modes. It became clear that the proposed detector is useful for micro-HPLC of carbohydrates in both separation modes.

The proposed detector was successfully applied to several real samples such as

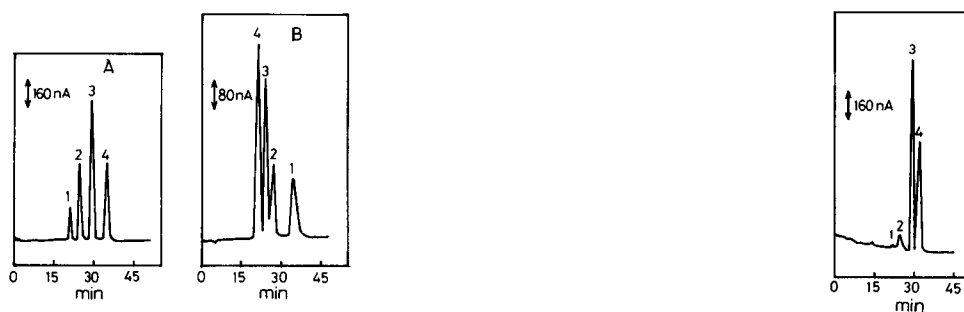


Fig. 9. Application to the detection of sugars separated by micro-HPLC in different modes. (A) Size-exclusion mode. Column, Shodex Ionpak KS-801 (247 mm  $\times$  0.35 mm I.D. + 217 mm  $\times$  0.35 mm I.D.); column temperature, 80°C. (B) Ion-exchange mode. Column, SAX (100 mm  $\times$  0.25 mm I.D. + 100 mm  $\times$  0.25 mm I.D.); column temperature, 30°C. Peaks: 1 = raffinose; 2 = lactose; 3 = glucose; 4 = arabinose. Amount of sample injected, 1.0 nmol each; flow-rates of water and 0.25 M NaOH, both 1.1  $\mu$ l/min; detection temperature, 60°C.

Fig. 10. Application to the detection of sugars in a real sample. Sample, 0.02  $\mu$ l of 4.40% honey; column, Shodex Ionpak KS-801 (247 mm  $\times$  0.35 mm I.D. + 217 mm  $\times$  0.35 mm I.D.); column temperature, 80°C. Peaks: 1 = raffinose; 2 = sucrose; 3 = glucose; 4 = fructose.

honey, cola and orange juice. Fig. 10 shows a typical chromatogram obtained for honey. In this instance, the sample was diluted with distilled water and injected directly onto the micro-column without any pretreatment. Hence the proposed detector can be applied to real samples without interferences from other analytes and eluent matrices present.

## REFERENCES

- 1 S. Hughes and D. C. Johnson, *Anal. Chim. Acta*, 132 (1981) 11.
- 2 S. Hughes and D. C. Johnson, *J. Agric. Food Chem.*, 30 (1982) 712.
- 3 S. Hughes and D. C. Johnson, *Anal. Chim. Acta*, 149 (1983) 1.
- 4 G. G. Neuburger and D. C. Johnson, *Anal. Chem.*, 59 (1987) 203.
- 5 P. Edwards and K. K. Haak, *Am. Lab.*, April (1983) 78.
- 6 R. D. Rocklin and C. A. Pohl, *J. Liq. Chromatogr.*, 6 (1983) 1577.
- 7 G. G. Neuburger and D. C. Johnson, *Anal. Chem.*, 59 (1987) 150.
- 8 K. G. Schick, V. G. Magearu and C. O. Huber, *Clin. Chem.*, 24 (1978) 448.
- 9 W. Buchberger, K. Winsauer and C. H. Breitwieser, *Fresenius' Z. Anal. Chem.*, 315 (1983) 518.
- 10 R. E. Reim and R. M. Van Effen, *Anal. Chem.*, 58 (1986) 3203.
- 11 Y. B. Vassilev, O. K. Khazova and N. N. Nikolaeva, *J. Electroanal. Chem.*, 196 (1985) 127.
- 12 L. M. Santos and R. P. Baldwin, *Anal. Chem.*, 59 (1987) 1766.
- 13 L. M. Santos and R. P. Baldwin, *Anal. Chim. Acta*, 206 (1988) 85.
- 14 S. V. Prabhu and R. P. Baldwin, *Anal. Chem.*, 61 (1989) 852.
- 15 M. Goto, K. Shimada, T. Takeuchi and D. Ishii, *Anal. Sci.*, 4 (1988) 17.
- 16 M. Fleischmann, K. Korinek and D. Pletcher, *J. Chem. Soc., Perkin Trans.*, 2 (1972) 1396.
- 17 G. G. Neuburger and D. C. Johnson, *Anal. Chim. Acta*, 192 (1987) 205.